Oxygen Vacancy Clustering and Electron Localization in Oxygen-Deficient $SrTiO_3$: LDA + U Study

Do Duc Cuong,[1] Bora Lee,[2] Kyeong Mi Choi,[1] Hyo-Shin Ahn,[3] Seungwu Han,[2,†] and Jaichan Lee[1,*]

[1]*School of Materials Science & Engineering, SungKyunKwan University, Suwon 440-746, Korea*
[2]*Department of Physics, Ewha Womans University, Seoul 120-750, Korea*
[3]*Future Technology Research Division, Korea Institute of Science and Technology, Seoul 136-791, Korea*

(Received 21 February 2006; published 15 March 2007; publisher error corrected 16 March 2007)

We find, using a local density approximation +Hubbard U method, that oxygen vacancies tend to cluster in a linear way in $SrTiO_3$, a prototypical perovskite oxide, accompanied by strong electron localization at the 3d state of the nearby Ti transition metal ion. The vacancy clustering and the associated electron localization lead to a profound impact on materials properties, e.g., the reduction in free-carrier densities, the appearance of characteristic optical spectra, and the decrease in vacancy mobility. The high stability against the vacancy migration also suggests the physical reality of the vacancy cluster.

DOI: 10.1103/PhysRevLett.98.115503 PACS numbers: 61.72.Bb, 61.72.Ji, 71.15.Mb, 77.84.Dy

Perovskite oxides with transition metal ions have been known to exhibit a wide variety of physical properties such as high dielectric constant, ferroelectric polarization, colossal magneto-resistance, superconductivity, and hence become a key material for oxide-based electronic devices [1]. The physical properties of the perovskite oxides have been extensively modified by introducing various defects. Among them, the self-doping by oxygen vacancies is of essence since the oxygen vacancy is one of the fundamental and intrinsic defects in perovskite oxides and gives a critical impact on their properties. For example, the oxygen vacancy in $SrTiO_3$ is known to dope the material with electron carriers, causing insulator-to-metal transition [2], further superconductivity at low temperatures [3], and changing optical properties to be visible-light emitting [4]. Therefore, the oxygen vacancy in oxides has been subject to various studies in theoretical and experimental aspects [5,6]. The oxygen vacancy defect is also known to be responsible for the degradation or failure of perovskite oxide-based devices [7,8]. Moreover, the oxygen vacancy is easily introduced into the perovskite oxides via various processes such as growth, annealing, and redox reactions.

The oxygen vacancy has been considered to exist in the form of a single isolated defect. However, experimental evidences have been accumulated to allow the possibility of vacancy clustering. It is reported that the carrier densities in oxygen-deficient $SrTiO_3$ were lower than expected one assuming the single isolated defect [9]. The transmission electron microscopy on $(SrTiO_3)_m(SrTiO_{3-\delta})_n$ superlattices showed a clear sign of defect clustering [10]. Vacancy ordering was also reported in degraded $BaTiO_3$ [11]. Since the vacancy clustering influences not only electrical properties but also the stability of defect-engineered oxides, the fundamental understanding is critical for further progress toward all-oxide electronic devices. However, there are few theoretical efforts [12] to study the microscopic structure of vacancy clusters, while many computational studies [13–17] were carried out for an isolated single vacancy.

In this Letter, we address vacancy-vacancy interaction in the perovskite oxide with an emphasis on the relative stability and the electronic structures by first-principles calculation with the correction of on-site Coulomb interaction (i.e., LDA + U). To our best knowledge, this is the first attempt to study the multiple vacancies in the perovskite with fully relaxed structures. We have chosen $SrTiO_3$ as a model system since it is a representative perovskite oxide with a wide range of physical properties from insulating to metallic or even superconducting upon compositional doping of various defects. Our computational results show that the oxygen vacancy tends to order in a linear way. The oxygen divacancy becomes stable when a linear pair of oxygens around a Ti atom is removed in the oxygen octahedron. Simultaneously, the localized in-gap state is identified, which becomes to successfully explain current experimental reports on transport and optical properties of $SrTiO_{3-\delta}$.

In choosing the computational framework, we note that the electrons can be trapped at a certain Ti atom, which would substantially increase its d-orbital occupancy. The electron occupation of Ti-3d orbital requires a careful treatment. A good example is the $LaTiO_3$, a well-known Mott insulator, with all Ti atoms in d^1 configuration. Contrary to the local-density approximation (LDA) or generalized gradient approximation (GGA), the LDA + U approach properly describes the localization nature of d electrons and shows an energy gap comparable to the experimental data [18–20]. Therefore, we employ the LDA + U approach to address the possible d^1 or d^2 configurations of Ti atoms in the electron-doping environment by oxygen vacancies. As will be detailed in the below, the LDA + U approach has a profound effect on the energetics of vacancy-vacancy interaction.

For the first-principles density functional calculations, we use the Vienna *Ab initio* Simulation Package (VASP)

[21]. The ionic potentials including the effect of core electrons are described by the projector augmented wave (PAW) method [22]. The plane waves with the kinetic energy up to 400 eV have been employed to expand the electronic wave functions. For calculating oxygen vacancies, we employ a $4 \times 4 \times 4$ supercell based on cubic $Pm3m$ perovskite structure which is a stable phase of $SrTiO_3$ at room temperature. The Brillouin-zone (BZ) integration is carried out using $2 \times 2 \times 2$ Monkhorst-Pack grid in the first BZ of the cubic supercell. The structural relaxations are performed until the Hellmann-Feynman force on each atom reduces within 0.05 eV/Å. For the exchange and correlation energy between electrons, we use LDA + U method with a rotationally invariant approach [23] as implemented within the package. Two set of Coulomb (U) and exchange (J) parameters are chosen for Ti-d orbitals; $U = 3.2$ eV, $J = 0.9$ eV [18] or $U = 5.0$ eV, $J = 0.64$ eV [19]. The LDA + U method applied on crystalline $SrTiO_3$ is found to increase its band gap up to 2.57 eV, compared to the LDA value of 1.72 eV [20]. (The experimental value is 3.3 eV.) The electronic structure of $LaTiO_3$ computed within the present LDA + U method also confirms the Mott insulating behavior with 0.2–0.5 eV optical gap, consistent with other literatures [18,20].

We first calculated on $SrTiO_3$ with the single oxygen vacancy in the LDA scheme. The density of states (DOS) indicates that two electrons are occupying the conduction bands with extended characters. No defect state associated with the oxygen vacancy is identified within the energy gap. On the other hand, when the LDA + U approach is used, a localized state is obtained in the band gap at a relatively large U parameter (for example, $U = 5.0$ eV, $J = 0.64$ eV), although it is shallow below the conduction band minimum by 0.11 eV. When the oxygen is further singly ionized, the localized level becomes deep (0.37 eV from the conduction band minimum). This localized state allows a good explanation on an experimental fact that the carrier density n is equal to the oxygen-vacancy concentration $[V_O^{\cdot}]$ (i.e., $n \sim [V_O^{\cdot}]$ or δ) in $SrTiO_{3-\delta}$ [24]. However, there has been an additional experimental report that the carrier density further decreased below δ as the oxygen-vacancy concentration δ increased significantly [9], which cannot be explained by the isolated single vacancy. Therefore, we carried out calculations on $SrTiO_3$ with two oxygen vacancies within the unit supercell in order to address the possible vacancy-vacancy interaction. This corresponds to the nominal stoichiometry of $SrTiO_{2.97}$, i.e., $\delta = 0.03$. The various configurations between two vacancies were thoroughly investigated. In Fig. 1, we show the interaction energies of some representative configurations as defined below.

$$E_{\text{int}} = E_{\text{tot}}(2V_O) + E_{\text{tot}}(0V_O) - 2E_{\text{tot}}(1V_O), \qquad (1)$$

where nV_O means that there are n oxygen vacancies within the supercell. The sign of E_{int} indicates whether the interaction is repulsive or attractive, although the precise assignment can be affected by the long-range relaxation of the oxygen vacancy [17].

In Fig. 1, it is noticeable that the energy of a divacancy with a Vac-Ti-Vac configuration is sensitive to the applied computational approaches. We call this configuration "apical divacancy", meaning that two apical oxygen atoms around the Ti atom are removed. Within the LDA method, the apical divacancy is higher in energy than other configurations. This is largely due to the fact that the relaxation of the Ti atom between the oxygen vacancies is partly prohibited along the Vac-Ti-Vac direction (i.e., z direction) by the symmetry. The relaxation energies, defined by the amount of lowered energy after relaxation from the bulk positions, are ≥ 3.0 eV for most configurations except for the apical divacancy where the energy is lowered by only $\sim$1.5 eV after structural relaxation. Despite the small degree of energy lowering from the relaxation, the apical divacancy configuration exhibits the large shift (decrease) of the energy, compared with other divacancy configurations, when LDA + U is applied. The large influence of the LDA + U approach is related to the presence of the localized state that will be detailed below.

In Fig. 2(a), we plot the band structures of the cubic supercell for the apical divacancy calculated with $U - J = 2.3$ eV. The localized state with flat band dispersion is found with the energy level located at 0.6 eV below the

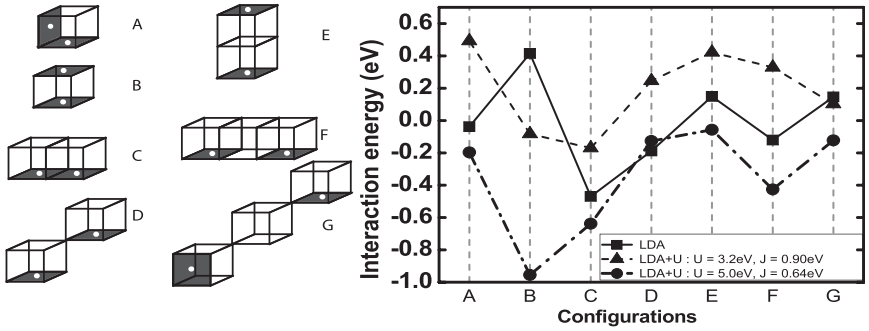

FIG. 1. The relative energy or interaction energy of representative divacancies. The configurations are shown in the increasing order of Vac-Vac separations. On the left, the schematic configuration of divacancy is shown. Each cube corresponds to the unit cell of crystalline $SrTiO_3$. The shaded faces indicate where the oxygen atoms (blank circles) are removed.

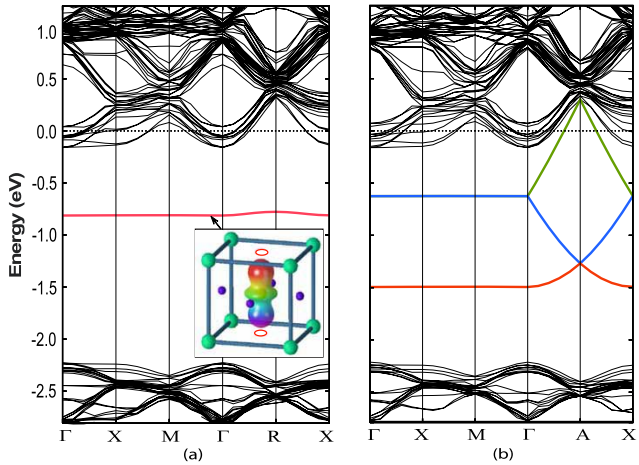

FIG. 2 (color online). (a) Band structure of the apical divacancy aligned along the z direction. The inset describes the squared wave function of the localized state which shows the Ti-$3d_{3z^2-r^2}$ characters. The open circles represent the oxygen vacancy. (b) Band structure of a linear cluster where four oxygens are removed from the lattice in the linear way along the Ti-Vac 001 direction.

conduction minimum. This in-gap state appears regardless of LDA or LDA + U, but the location of this state varies from 0.3 eV (LDA) up to 1.14 eV ($U - J = 4.36$ eV). On the other hand, other configurations of divacancies considered do not show such a localized state within the energy gap. The Fermi level lies in the conduction band, implying that the localized state is doubly occupied. The isosurface of the squared wave function of the localized state is plotted in the inset of Fig. 2(a). It can be seen that the state is mostly localized around the Ti atom between the oxygen vacancies and the spatial distribution shows the Ti-$3d_{3z^2-r^2}$ character, which leads to d^2 configuration of the Ti atom. The effectively positive potential of the oxygen vacancy contributes to stabilize the energy level of nearby Ti-$3d$ orbitals. The $3d_{3z^2-r^2}$ orbital of the closest Ti atom is under the biggest influence because of its symmetry with the apical divacancy. In other words, the maximum density of the Ti-$3d_{3z^2-r^2}$ orbital is pointing toward two oxygen vacancies above and below the Ti atom since the Ti ion is fixed, i.e., unrelaxed, and preserves the symmetric position for the apical oxygen divacancy.

In fact, the structural relaxation is crucial to the existence of localization of d electrons. At the A configuration in Fig. 1, without allowing ionic relaxation, we found a localized state below the conduction band similar to that reported in Ref. [12]. However, allowing ionic relaxation leads to the upward shift of the localized state above the Fermi level and further delocalization of the state. On the other hand, the fixed position of Ti and the symmetric configuration in the apical divacancy retain the localized state in the band gap despite of the shift in the gap state. The corresponding distance of Ti from the oxygen vacancy is small compared to the other divacancy configurations, further favoring the localization of d electrons.

The location of localized levels at 0.6 eV ($U - J = 2.3$ eV) below the conduction band minimum is consistent with the ionization energy of the oxygen vacancy estimated in experiment [25]. We also note that the energy level of the localized state from the valence top is 2.7 eV if the experimental band gap of 3.3 eV is considered. This is in good comparison with blue-light emission at 2.8 eV found in the oxygen-deficient layers of $SrTiO_3$ [4], suggesting that the existence of the oxygen-vacancy cluster, i.e., divacancy, could be an explanation of the observed photoluminescence properties of $SrTiO_{3-\delta}$.

Now one can understand why the LDA + U method shows a large energy shift only for the apical divacancy. One effect of the LDA + U method is the correction of the spurious self-interaction of the localized orbital that is undesirably included in the LDA results. The overestimation of Coulombic energies severely affects the relative energy of defects that create the occupied localized levels. The application of LDA + U method corrects it, albeit in an empirical manner. This is consistent with the fact that increasing the U value lowers further the relative energy of the apical divacancy. It is worth a comment on how to choose U and J parameters. As is found in the literature, the on-site Coulomb energy is largely dependent on the screening scheme used in the constrained density functional calculation while the exchange J parameter is fixed at $\sim$1 eV. The large values of U from 5 up to 8 eV are obtained assuming the localization of all d electrons of Ti atom while the screening by e_g orbital substantially reduces U parameter of t_{2g} level down to 3.2 eV [18]. In fact, the situation in the apical divacancy does not exactly match with any of these assumptions. The e_g level, rather than t_{2g} ones, is localized [shown in Fig. 2(a)] and the screening of t_{2g} level is less efficient than e_g level due to the large effective mass. On the other hand, the doubly occupied e_g means that the wave function will slightly expand, reducing the on-site Coulomb energy [close to $U(M^{2+})$ configuration in Ref. [18]]. Considering the above all together, a reasonable choice of the U parameter in our situation would lie between 3 and 5 eV.

For high defect densities, we created two apical divacancies from the $4 \times 4 \times 4$ supercell. Among the several configurations tested, the one with four oxygen vacancies lying along the [001] direction in the TiO_2 plane (i.e., linear cluster) is found to be most stable, exhibiting also localized states with mainly Ti $3d_{3z^2-r^2}$ character, which leads to d^2 configuration of the Ti atom. The band structure [shown in Fig. 2(b)] indicates that most of electrons transferred from oxygen vacancies are localized at the Ti atoms along the vacancy chain. Since the localized state appearing in the apical divacancy forms a trap level, only two electrons are counted as free carriers among four electrons released from the divacancy. Assuming that all the vacancies are paired in this configuration, the carrier density will be reduced to δ. This carrier density will decrease even further if linear vacancy chains appear at highly oxygen

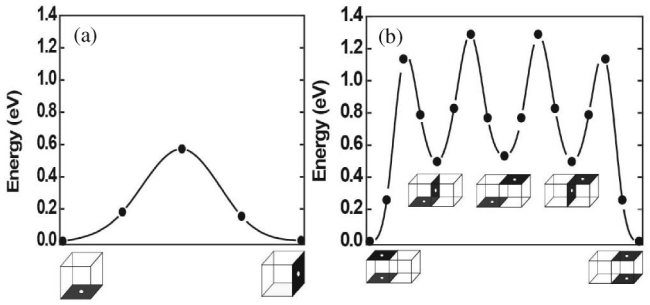

FIG. 3. The migration barriers of (a) single oxygen vacancy and (b) apical divacancy in concerted moving to the next position in the lateral direction. The energy profile is calculated by using NEB method with $U - J = 2.3$ eV.

deficiencies. In fact, the Hall measurement performed on $SrTiO_{3-\delta}$ with δ ranging from 0.08 to 0.28 showed that the actual carrier concentration was in the range from $\delta/2$ to δ per unit volume [9]. Those results could be well explained by localized states in divacancy and linear vacancy chain and suggest the possibility of oxygen-vacancy clustering.

Further, we compare the energy barrier of single oxygen vacancy and apical divacancy migration to a neighboring location. We employed the nudged-elastic band (NEB) method [26] to calculate the minimum energy barrier. Because of the steep computational demand, we employ a smaller $3 \times 3 \times 3$ supercell. In the case of apical divacancy, we chose minimum number of intermediate configurations and calculated the energy barriers between them. We put three replicas between the local minima. The computed migration barrier of 0.6 eV for the single vacancy diffusion is in reasonable agreement with experimental values of 0.67–1.27 eV [27]. The migration path for the divacancy is shown in Fig. 3(b) and represents one of the shortest possible paths moving in xy plane. We find that the maximum barrier along the diffusion path occurs at the first step with the barrier of 1.2 eV, much larger than that of isolated single vacancy. The increase in the barrier reflects the energy difference between the apical divacancy and the nearest-neighbor vacancy pair (configuration A in Fig. 1). The increase in the migration barrier as well as the multiple steps again suggests the stable configuration of the oxygen-vacancy cluster in $SrTiO_{3-\delta}$.

In conclusion, the oxygen-vacancy linear cluster and its associated electron localization have been successfully addressed by LDA + U. The linear vacancy cluster and the appearance of the in-gap states explain many experimental results such as transport behaviors and photoluminescence of oxygen-deficient $SrTiO_3$, which may provide a viable route to understand various physical behaviors, specifically transport properties, of the perovskite oxide that is inherently prone to oxygen nonstoichiometry. Our results also suggest that material properties can be substantially influenced by the vacancy clusters through the region such as interface or grain boundary where the nonstoichiometry is often enhanced.

This work was supported by the National Program for 0.1 Terabit NVM Devices and Korean Science and Engineering Foundation (KOSEF) through the National Research Laboratory (NRL) Program and CAPST. The computations were carried out at KISTI through the 8th Strategic Supercomputing Program.

*Corresponding author.
Electronic address: jclee@skku.edu
†Electronic address: hansw@ewha.ac.kr

[1] *Thin Films and Heterostructures for Oxide Electronics*, edited. by S. B. Oagle (Springer, New York, 2005).
[2] P. Calvani *et al.*, Phys. Rev. B **47**, 8917 (1993).
[3] J. F. Schooley, W. R. Hosler, and M. L. Cohen, Phys. Rev. Lett. **12**, 474 (1964).
[4] D. Kan *et al.*, Nat. Mater. **4**, 816 (2005).
[5] J. Carrasco *et al.*, Phys. Rev. Lett. **93**, 225502 (2004).
[6] K. Szot *et al.*, Phys. Rev. Lett. **88**, 075508 (2002); C. L. Jia *et al.*, *ibid.* **95**, 225506 (2005).
[7] G. Y. Yang *et al.*, J. Appl. Phys. **94**, 5990 (2003).
[8] J. F. Scott, *Ferroelectric Memories* (Springer, New York, 2000).
[9] W. Gong *et al.*, J. Solid State Chem. **90**, 320 (1991).
[10] D. A. Muller *et al.*, Nature (London) **430**, 657 (2004).
[11] D. I. Woodward *et al.*, Appl. Phys. Lett. **84**, 4650 (2004).
[12] N. Shanthi and D. D. Sarma, Phys. Rev. B **57**, 2153 (1998).
[13] R. Astala and P. D. Bristowe, Model. Simul. Mater. Sci. Eng. **9**, 415 (2001).
[14] T. Tanaka *et al.*, Phys. Rev. B **68**, 205213 (2003).
[15] D. Ricci, G. Bano, and G. Pacchioni, Phys. Rev. B **68**, 224105 (2003).
[16] W. Luo, W. Duan, S. G. Louie, and M. L. Cohen, Phys. Rev. B **70**, 214109 (2004).
[17] J. P. Buban, H. Iddir, and S. Öğüt, Phys. Rev. B **69**, 180102(R) (2004).
[18] I. Solovyev, N. Hamada, and K. Terakura, Phys. Rev. B **53**, 7158 (1996).
[19] E. Pavarini *et al.*, Phys. Rev. Lett. **92**, 176403 (2004).
[20] H. S. Ahn, D. D. Cuong, J. Lee, and S. Han, J. Korean Phys. Soc. **49**, 1536 (2006).
[21] G. Kresse and J. Hafner, Phys. Rev. B **47**, 558(R) (1993); **49**, 14 251 (1994).
[22] P. E. Blöchl, Phys. Rev. B **50**, 17 953 (1994). The valence configurations are chosen as $4s^2 4p^6 5s^2$ for Sr atoms, $4s^1 3d^3$ for Ti atoms, and $2s^2 2p^4$ for O atoms.
[23] S. L. Dudarev *et al.*, Phys. Rev. B **57**, 1505 (1998).
[24] R. Moos *et al.*, Appl. Phys. A **61**, 389 (1995).
[25] I. P. Raevski *et al.*, J. Phys. Condens. Matter **10**, 8015 (1998).
[26] G. Mills, H. Jonsson, and G. K. Schenter, Surf. Sci. **324**, 305 (1995).
[27] A. E. Paladino *et al.*, J. Phys. Chem. Solids **26**, 391 (1965); A. Yamaji, J. Am. Ceram. Soc. **58**, 152 (1975).